Stereoselection

DOI: 10.1002/ange.201206011

Stereoselection in the Corey–Bakshi–Shibata Reduction: Insight from Kinetic Isotope Effects and Transition-Structure Modeling**

*Hui Zhu, Daniel J. O'Leary, and Matthew P. Meyer**

The Corey–Bakshi–Shibata (CBS) reduction is one of the most versatile methods for the enantioselective reduction of prochiral ketones, exhibiting both high selectivity and a large substrate range.[1] Enantiofacial discrimination depends upon the effective discrimination of the large (R_L) and small (R_S) substituents (Scheme 1). Steric repulsion is accepted as a key director of stereoselection; however, direct measures of steric interaction at the transition state (TS) are difficult to obtain.[2] Steric kinetic isotope effects (KIEs) offer a means of investigating steric interactions quantitatively.[3] Herein, we leverage a combined experimental and computational approach toward answering the following questions regarding stereoselection in the CBS reduction of 2′,5′-dimethylisobutyrophenone (**1**) using the oxazaborolidine (**2**) as a catalyst. 1) Is it reasonable to assume that steric repulsion develops only at the small carbonyl substituent (R_S) during enantiofacial discrimination? 2) How can steric KIEs be distinguished from KIEs arising from other factors? 3) How severe are conformational constraints in reactions that take place via cyclic transition structures?

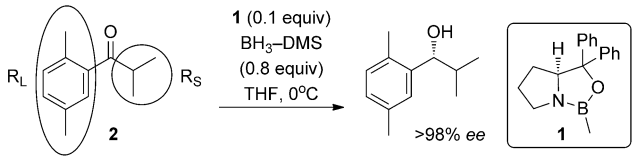

Scheme 1. CBS reduction of 2′,5′-dimethylisobutyrophenone. DMS = dimethyl sulfide.

Using a modification of a previously reported method (see Experimental Section), we measured the ^{2}H KIEs at the 2′- and 5′-methyl positions within **1**.[4] We also computed the ^{13}C KIE at the carbonyl position and the ^{2}H KIEs at the pro-*R*, pro-*S*, 2′-, and 5′-methyl positions within **1** by using optimized reactant and transition structures to compare with previously measured values.[5,6] Two distinct conformeric transition structures (chair-like and boat-like) were optimized for the CBS reduction of **1** (Figure 1). The more stable conformer (2.39 kcal mol^{-1}) exhibits a chair-like configuration of the six "active" atoms. Computed KIEs that result from both transition structures are reported alongside experimentally determined KIEs (Table 1). Three results are immediately apparent from comparisons of the experimental and computational data. First, the ^{2}H KIEs measured at the prochiral methyl groups and the 2′-methyl position are substantial and inverse ($k_H/k_D < 1$). Second, computed KIEs, with the possible exception of the effect observed at the pro-*R* methyl group, are in excellent accord with measured KIEs. Third, KIEs computed from transition structures with chair-like and boat-like arrangements of the six "active" atoms do not differ significantly. Explaining the physical origins of each of these observations will provide some insight into the interpretation of ^{2}H KIE measurements in stereoselective reactions and provide a unified conceptual understanding of the inherent properties of oxazaborolidine-catalyzed reductions.

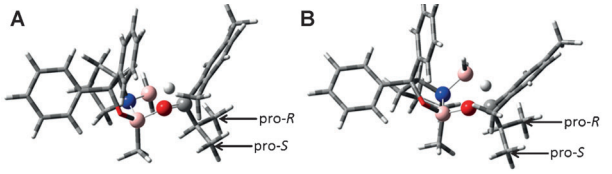

Figure 1. Optimized [B3LYP/6-31 + G(d,p)] structures for A) chair-like and B) boat-like transition structures. Cyclic arrangements of reactive atoms are shown as color-coded spheres (N: blue, O: red, B: pink, C: gray, and H: white).

Table 1: Comparison of experimentally determined KIEs and those computed from optimized reactant and transition structures.

	C=O[a]	pro-*R*[b,c]	pro-*S*[b,c]	2′-Me[b]	5′-Me[b]
Experiment	1.025(1)	0.965(3)	0.974(3)	0.980(5)	0.995(5)
Chair-like TS[d,f]	1.023	0.944	0.972	0.973	0.993
Chair-like TS[e,f]	1.029	0.951	0.966	0.974	0.998
Boat-like TS[d,f]	1.024	0.938	0.962	0.978	0.999
Boat-like TS[e,f]	1.030	0.947	0.970	0.981	1.000

[a] ^{13}C KIE; Ref. [6]. [b] ^{2}H KIE (CH_3/CD_3). [c] Ref. [5]. [d] Computed at B3LYP/6-31 + G(d,p). [e] Computed at B3LYP/6-31 + G(d,p) with IEFPCM model for THF solvent. [f] Computed using the Bigeleisen equation with scaled frequencies and a Bell tunnel correction.

It seems reasonable to expect that methyl positions giving significant inverse ^{2}H KIEs as a result of steric repulsion would display greater rotational barriers in computed tran-

[*] Prof. M. P. Meyer
Department of Chemistry, University of California, Merced
Merced, CA 95343 (USA)
E-mail: mmeyer@ucmerced.edu
Prof. D. J. O'Leary
Department of Chemistry, Pomona College
Claremont, CA 91711 (USA)
Dr. H. Zhu
Department of Chemistry, University of California, Berkeley
Berkeley, CA 94720 (USA)

[**] M.P.M. acknowledges support from the NSF (CHE-1058483 and CHE-0840505). D.J.O. thanks Pomona College for supporting this research.

Supporting information for this article is available on the WWW under http://dx.doi.org/10.1002/anie.201206011.

sition structures than in computed reactant structures. In a series of computed relaxed rotor scans, the rotational barriers for the pro-*R* and pro-*S* methyl groups are indeed higher in the transition structure than in the reactant (Figure 2 A&B, respectively). By contrast, the rotational barrier decreases for the 2′-methyl position in going from the

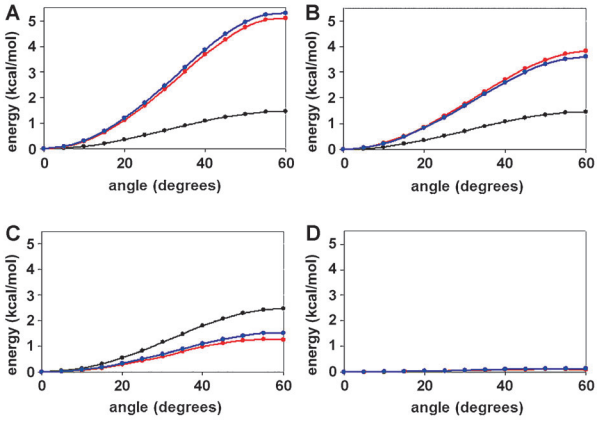

Figure 2. Methyl rotation profiles for reactant (black), chair-like transition structure (red), and boat-like transition structures (blue) corresponding to the A) pro-*R*, B) pro-*S*, C) 2′-, and D) 5′-positions.

optimized reactant structure to the transition structure (Figure 2 C). No significant potential energy barrier for rotation appears to exist in either the reactant or transition structure for the 5′-methyl group (Figure 2 D). This result might be expected, given the small barriers associated with methyl rotation in toluene ($\approx 14\,\mathrm{cal\,mol^{-1}}$).[7] Intuitively it seems reasonable to ascribe the origins of the ^{2}H KIEs at the prochiral methyl groups to steric origins, considering that the prochiral methyl groups are conjugatively isolated from the center of the reaction, that is, hyperconjugation effects seem unlikely. The scans for methyl rotation further suggest that, if anything, there should be a normal ($k_H/k_D > 1.0$) steric contribution to the ^{2}H KIE at the 2′-methyl position because steric repulsion appears to be relieved in the transition state for this position. Therefore, it is most reasonable to expect that the γ-^{2}H KIE at the 2′-methyl position arises largely from a reduction in hyperconjugation in going from the reactant to the transition state. This notion is supported by the observation that C–H bond lengths within the 2′-methyl rotor are longer in the optimized chair-like and boat-like transition structures than in the optimized reactant structure.

The conventional view of steric isotope effects holds that the C–D bond is effectively shorter than the C–H bond, resulting in inverse ^{2}H KIEs for reactions in which steric repulsion increases at the transition state.[3a,8] A recent report by Dunitz and Ibberson challenged this view by demonstrating that the unit cell of C_6D_6 is smaller than that of C_6H_6 below 170 K but larger than that of C_6H_6 above 170 K.[9] They further posited that the temperature dependence of the relative size of these isotopologs of benzene was likely due to low frequency vibrational modes, the contributions of which become more important at higher temperatures. In another recent report, O'Leary et al. used an enthalpy/entropy decomposition of the computed ^{2}H KIE for the stereoinversion of two axially chiral molecules to demonstrate that ^{2}H KIEs that arise from the development of significant repulsive interactions at the transition state give significant normal ($k_H/k_D > 1$) entropic contributions and inverse ($k_H/k_D < 1$) enthalpic contributions to the KIE.[10] Analogous with the findings from Dunitz and Ibberson, O'Leary et al. found that entropic contributions to the KIE can outweigh enthalpic contributions, leading to an overall normal ^{2}H KIE. Enthalpy/entropy analyses of computed ^{2}H KIEs offer another view into the origins of the isotope effects measured here. In accordance with methyl rotational barriers, one might anticipate that enthalpy/entropy decompositions of the CH_3/CD_3 KIEs at the pro-*R* and pro-*S* positions give both significant normal entropic contributions and significant inverse enthalpic contributions. Results reported in Table 2 demonstrate that this is indeed the case. Compared to the pro-*S* methyl group, the pro-*R* methyl group exhibits larger (inverse) enthalpic and smaller (normal) entropic contributions to the KIE. Steric KIEs at the prochiral methyl positions offer a contrast to the KIE at the 2′-methyl position, which appears to be largely dominated by an enthalpic contribution. These two findings suggest a means of assigning the origins of the substantial inverse ^{2}H KIEs at the pro-*R*, pro-*S*, and 2′-methyl groups shown in Table 1. In total, these results suggest that steric ^{2}H KIEs may have enthalpy/entropy contributions that differ from KIEs arising from stereoelectronic effects (e.g., hyperconjugation).

Table 2: Computational decompositions of ^{2}H KIEs into their enthalpic/entropic contributions.

	pro-*R*[a]	pro-*S*[a]	2′-Me[a]	5′-Me[a]
Experiment	0.965(3)	0.974(3)	0.980(5)	0.995(5)
		Chair-like transition structure		
$\Delta\Delta G^{\ddagger}$	0.955	0.971	0.974	0.998
$\Delta\Delta H^{\ddagger}$	0.925	0.946	0.973	0.995
$-T\Delta\Delta S^{\ddagger}$	1.032	1.026	1.001	1.002
		Boat-like transition structure		
$\Delta\Delta G^{\ddagger}$	0.950	0.974	0.978	1.000
$\Delta\Delta H^{\ddagger}$	0.920	0.957	0.978	1.000
$-T\Delta\Delta S^{\ddagger}$	1.032	1.018	1.000	1.000

[a] ^{2}H KIE (CD_3/CH_3). [b] Computed at B3LYP/6-31+G(d,p) with an IEFPCM model for THF solvent, unscaled frequencies, and no tunnel correction.

What is perhaps most striking about the information in Tables 1 and 2 and Figures 1 and 2 is that chair-like and boat-like transition structures appear quite similar in all respects. The structural similarities between these two transition structures are evident in a maximal overlap superposition (Figure 3). Though the boat-like transition structure appears to place the isopropyl substituent (R_S) of **1** in a more axially confined environment than in the chair-like transition structure, the borane moiety is removed to a position that is approximately 0.3 Å more distant from the pro-*R* methyl

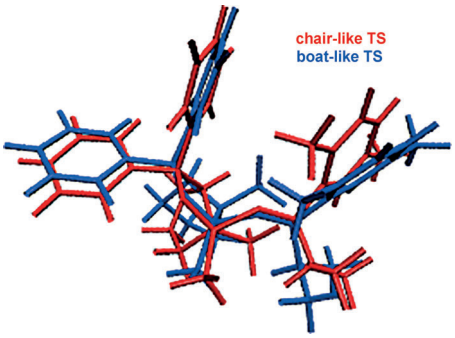

Figure 3. Overlay of computed [B3LYP/6-31 + G(d,p)] chair-like (red) and boat-like (blue) transition structures.

group. Given the rotational barriers for the pro-*R* methyl group and the computed KIEs, it appears that this steric trade-off is nearly equivalent. Taken as a whole, the physical and structural similarities between the chair-like and boat-like transition structures suggest a flexible means of enforcing stereoselection. The chair-like transition structure is computed to be 2.39 kcal mol^{-1} lower in free energy than the boat-like transition structure. While this value cannot be considered quantitatively reliable, it points to the possibility that **2** can potentially enforce stereoselection through a conformationally diverse set of transition structures, depending upon the steric demands presented by the substrate. While this viewpoint is at variance with the conclusions of previous computational studies of the CBS reaction, it is consonant with the extensive substrate range observed for reductions catalyzed by **2**.[11]

In summary, we have found that the transition state for the highly enantioselective borane reduction of **2** catalyzed by **1** involves steric interactions only at the smaller (isopropyl) substituent. We have also illustrated two computational methods by which steric ^{2}H KIEs may be differentiated from those arising from other physical origins. KIEs that are measured at the methyl groups and arise from steric interactions exhibit rotational barriers that increase at the transition state. Steric KIEs also appear to exhibit substantial normal contributions as a result of entropy, while KIEs that arise from hyperconjugation do not have large entropic contributions. The result of our experimental and computational work is a conceptual understanding of the origins of the large substrate range exhibited by **1** in enantioselective reductions. The key feature of our conceptual model is the notion that, although the CBS reduction proceeds via a cyclic transition structure, which is generally assumed to enforce rigidity, stereoselection can likely be mediated through a flexible transition structure that conforms to the steric requirements of the substrate.

Methods Section

Experimental measurements of ^{2}H KIEs at the 2′- and 5′-methyl positions on **1** were achieved using a variation of a previously published methodology.[4] Two competition reactions were used, in conjunction with the rule of the geometric mean, to extract individual ^{2}H KIEs at the 2′- and 5′-methyl positions. The first competition reaction, which used [2′-D$_3$]-**1** and [5′-D$_3$]-**1** as competing substrates, gives the relative rates for the reduction of these isotopomers, KIE$_R$ [Eq. (1)]. Six measurements of the relative rates for the

$$\mathrm{KIE_R} = \frac{k_{2'-\mathrm{D3}}}{k_{5'-\mathrm{D3}}} = \frac{k_{\mathrm{H6}}}{k_{5'-\mathrm{D3}}} \Big/ \frac{k_{\mathrm{H6}}}{k_{2'-\mathrm{D3}}} \quad (1)$$

reduction of [2′-D$_3$]-**1** and [5′-D$_3$]-**1** were performed. The second competition reaction employed **1** and [D$_6$]-**1** as competing substrates. The ratio of rates for the reduction of **1** and [D$_6$]-**1** gave the product of the KIEs at the 2′- and 5′-positions, KIE$_P$ [Eq. (2)]. Four measurements of the relative rates for

$$\mathrm{KIE_P} = \frac{k_{\mathrm{H6}}}{k_{\mathrm{D6}}} = \frac{k_{\mathrm{H6}}}{k_{5'-\mathrm{D3}}} \times \frac{k_{\mathrm{H6}}}{k_{2'-\mathrm{D3}}} \quad (2)$$

the reduction of **1** and [D$_6$]-**1** were performed. The rule of the geometric mean and simple algebra gave the ^{2}H KIEs at both the 2′- and 5′-methyl positions [Eqs. (3) and (4), respectively].[12] The synthesis of a mixture of [2′-D$_3$]-**1** and [5′-D$_3$]-**1** was achieved via Friedel–Crafts acylation of [D$_3$]-*p*-xylene.[13] Synthesis of [D$_3$]-*p*-xylene was achieved using Suzuki coupling of *p*-tolylboronic acid and CD$_3$I.[14] Synthesis of [D$_6$]-**1** was accomplished by employing the Friedel–Crafts acylation of [D$_6$]-xylene. Gaussian 09 was used to optimize reactant and transition structures and to compute vibrational frequencies resulting from optimized structures.[15] The bicyclic nature of the oxazaborolidine catalyst limits accessible conformational space to rotameric conformers involving rotations around the C–Ar bond in the transition structures. This conformational space was explored, and the reported conformers represent the only accessible saddle point structures for *Si* attack. Methyl rotation barriers were computed using a relaxed scan of one of the three dihedrals for which the C–CH$_3$ bond was the central bond. Enthalpic and entropic ^{2}H KIEs were computed using thermochemistry outputs from Gaussian 09.

$$\frac{k_{\mathrm{H6}}}{k_{2'-\mathrm{D3}}} = \sqrt{\mathrm{KIE_P}/\mathrm{KIE_R}} \quad (3)$$

$$\frac{k_{\mathrm{H6}}}{k_{5'-\mathrm{D3}}} = \sqrt{\mathrm{KIE_P} \times \mathrm{KIE_R}} \quad (4)$$

Received: July 26, 2012
Published online: October 16, 2012

Keywords: asymmetric catalysis · isotope effects · reaction mechanisms · stereoselection · steric repulsion

[1] a) E. J. Corey, R. K. Bakshi, S. Shibata, *J. Am. Chem. Soc.* **1987**, *109*, 5551–5553; b) E. J. Corey, R. K. Bakshi, S. Shibata, C.-P. Chen, V. K. Singh, *J. Am. Chem. Soc.* **1987**, *109*, 7925–7926; c) E. J. Corey, S. Shibata, R. K. Bakshi, *J. Org. Chem.* **1988**, *53*, 2861–2863; d) E. J. Corey, *Pure Appl. Chem.* **1990**, *62*, 1209–1216; e) E. J. Corey, C. J. Helal, *Angew. Chem.* **1998**, *110*, 2092–2118; *Angew. Chem. Int. Ed.* **1998**, *37*, 1986–2012.
[2] T. Giagou, M. P. Meyer, *Chem. Eur. J.* **2010**, *16*, 10616–10628.

[3] a) R. E. Carter, *Adv. Phys. Org. Chem.* **1973**, *10*, 1 – 27; b) T. Felder, C. A. Schalley, *Angew. Chem.* **2003**, *115*, 2360 – 2363; *Angew. Chem. Int. Ed.* **2003**, *42*, 2258 – 2260; c) T. Hayama, K. K. Baldridge, Y.-T. Wu, A. Linden, J. S. Siegel, *J. Am. Chem. Soc.* **2008**, *130*, 1583 – 1591; d) J. S. Mugridge, R. G. Bergman, K. N. Raymond, *Angew. Chem.* **2010**, *122*, 3717 – 3719; *Angew. Chem. Int. Ed.* **2010**, *49*, 3635 – 3637.

[4] J. D. West, S. E. Stafford, M. P. Meyer, *J. Am. Chem. Soc.* **2008**, *130*, 7816 – 7817.

[5] M. P. Meyer, *Org. Lett.* **2009**, *11*, 4338 – 4341.

[6] J. Saavedra, S. E. Stafford, M. P. Meyer, *Tetrahedron Lett.* **2009**, *50*, 1324 – 1327.

[7] W. A. Kreiner, H. D. Rudolph, B. T. Tan, *J. Mol. Spectrosc.* **1973**, *48*, 86 – 99.

[8] a) L. S. Bartell, *Tetrahedron Lett.* **1960**, *1*, 13 – 16; b) L. S. Bartell, *J. Am. Chem. Soc.* **1961**, *83*, 3567 – 3571; c) L. S. Bartell, *Tetrahedron* **1962**, *17*, 177 – 190.

[9] J. D. Dunitz, R. M. Ibberson, *Angew. Chem.* **2008**, *120*, 4276 – 4278; *Angew. Chem. Int. Ed.* **2008**, *47*, 4208 – 4210.

[10] D. J. O'Leary, P. R. Rablen, M. P. Meyer, *Angew. Chem.* **2011**, *123*, 2612 – 2615; *Angew. Chem. Int. Ed.* **2011**, *50*, 2564 – 2567.

[11] a) D. K. Jones, D. C. Liotta, I. Shinkai, D. J. Mathre, *J. Org. Chem.* **1993**, *58*, 799 – 801; b) G. Alagona, C. Ghio, M. Persico, S. Tomasi, *J. Am. Chem. Soc.* **2003**, *125*, 10027 – 10039.

[12] J. C. Decius, E. B. Wilson, Jr., *J. Chem. Phys.* **1951**, *19*, 1409 – 1412.

[13] H. Zhu, M. P. Meyer, *Chem. Commun.* **2011**, *47*, 409 – 411.

[14] L. J. Gooßen, *Appl. Organomet. Chem.* **2004**, *18*, 602 – 604.

[15] Gaussian 09, Revision A.02, M. J. Frisch, et al., see the Supporting Information for the full reference.

